Computer Assisted Mechanics and Engineering Sciences, 7: 377–390, 2000.

Yttrium distribution in Ba–Cu–O melt during growth of superconducting material Y123 by Czochralski method

Janusz S. Szmyd, Krzysztof Gajek
University of Mining and Metallurgy, Mickiewicza 30, 30-059 Cracow, Poland

Kenjiro Suzuki
Kyoto University, Kyoto 606, Japan

(Received September 16, 1999)

Numerical computations of the yttrium distribution in the BaO–CuO melt were performed for the single crystal growth of yttrium barium copper oxide superconductor ($YBa_2Cu_3O_{7-x}$) with the Czochralski method. The finite volume method was used to calculate the fluid flow, heat transfer and yttrium distribution in the melt with staggered numerical grid. The flow in the melt was assumed to be axisymmetric and was modelled as an incompressible Newtonian, Boussinesque fluid. Mass transfer was due to both convection and diffusion. Calculations were presented for a buoyancy/crystal-rotation driven combined convective flow.

NOTATIONS

C_p – specific heat at constant pressure
g – acceleration due to gravity
Gr – Grashof number
H_l – depth of melt
P – static pressure
Pr – Prandtl number
r – radius
Re – Reynolds number
Sc – Schmidt number
t – time
T – temperature
U_i – component of velocity
r, φ, z – cylindrical–polar co-ordinates
C – concentration

Greek symbols

β – thermal expansion coefficient of the melt
λ – thermal conductivity
μ – molecular viscosity
ν – kinematics viscosity
ρ – density
Ω – angular velocity

Subscripts and superscripts

r, φ, z – cylindrical–polar co-ordinates
c – crucible
x – crystal
l – fluid
$*$ – dimensionless value

1. Introduction

Since 1987, when Wu *et al.* [15] discovered high temperature superconductivity at the temperature level of 90 K in a new mixed-phase compound system, an enormous amount of attention has been given to such compound systems. One of the most seriously studied compounds is the yttrium barium copper oxide superconductor $YBa_2Cu_3O_{7-x}$ (Y123).

Many processes, such as flux method and liquid phase epitaxy have been applied to produce single crystals of such compound systems to supply them for the measurement of physical properties or for electronic devices utilizing their superconductive properties, *e.g.* Hikada *et al.* [5], Dembinski *et al.* [2], Drake *et al.* [3], Gagnon *et al.* [4], Barilo *et al.* [1]. With these methods, the crystal nucleation in the melt cannot be controlled. Therefore it was difficult to stabilise the crystal growth and therefore to produce a large single crystal.

In 1993 Yamada and Shiohara [16] successfully grew an Y123 single crystal by applying a modification of the Czochralski method, which allows continuous crystal growth. The schematic configuration of the method is illustrated in Fig. 1. The Y_2BaCuO_5 (Y211) phase (green powder) was placed as a solute at the bottom of the crucible which was made of yttria (99.5% Y_2O_3 with 0.5% TiO_2) [17]. The solvent of BaO-CuO composite ($3BaCuO_2 \cdot 2CuO$) was put on the layer of the solute Y211 (the ratio Ba to Cu in the liquid was 3 to 5). The crucible was set in a conventional crystal pulling-up furnace (see Fig. 2). A resistance heater was placed to maintain the crucible side wall at a temperature appropriate but in a manner having a constant vertical temperature gradient. After melting the BaO–CuO composite completely, the temperature at the surface of the melt was about 1273 K. A MgO single crystal coated with Y123 thin film deposition was used as a seed crystal. The pulling rate was 0.5 mm/h and the rotation of the seed crystal was about 120 rpm. Temperature gradient in the melt was maintained to ensure that the temperature at the melt surface was lower

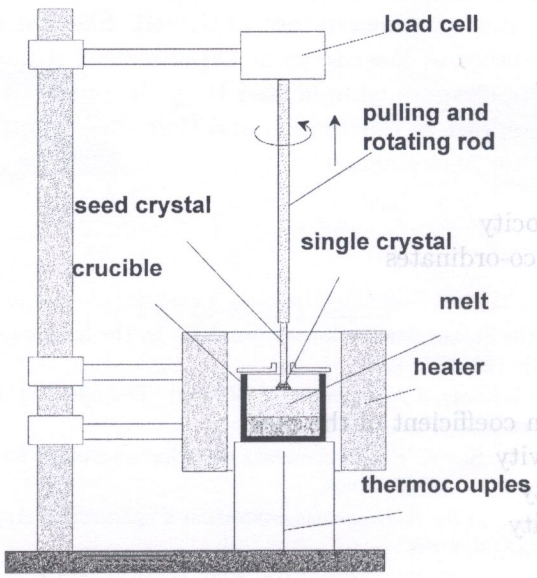

Fig. 1. System layout during the Y123 crystal growth

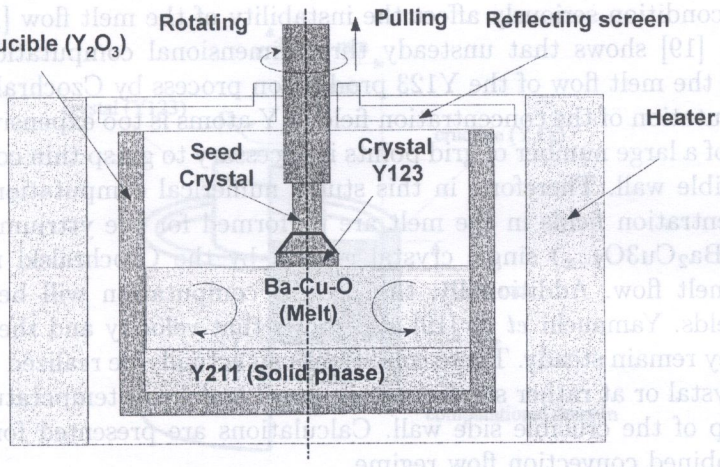

Fig. 2. Single crystal pulling furnace

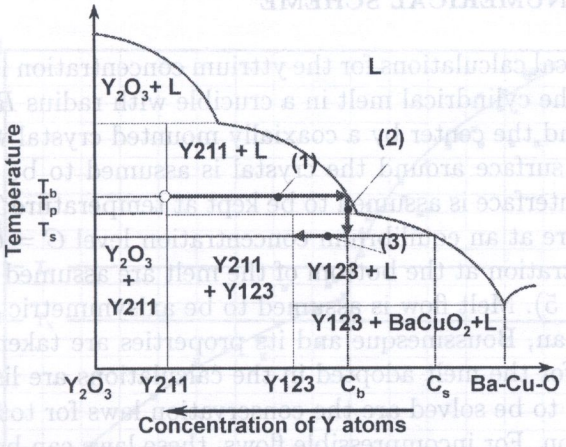

Fig. 3. The quasi-binary phase diagram of Y211–Y123–3$BaCuO_2$ · 2CuO, (T_b – temperature at the bottom of the melt, T_p – peritectic temperature of Y123, T_s – temperature at the melt surface), arrow (1) = Y211 ⟶ liquid (rich solution), arrow (2) = liquid (rich solution) ⟶ liquid (supersaturated), arrow (3) = liquid (supersaturated) ⟶ Y123

than the peritectic temperature of Y123 and that the temperature at the bottom of the melt was higher than the peritectic temperature of Y123 (see Fig. 3).

The quality of the crystal of yttrium barium copper oxide superconductor $YBa_2Cu_3O_{7-x}$ (Y123) grown from a melt by this method is significantly affected by heat and mass transfer in the melt during its growth process. In an Y123 single crystal growth system the Y123 single crystal grows directly from the BaO–CuO melt as a primary phase by migrating Y atoms transported from the solute Y_2BaCuO_5 (Y211) at the bottom of the melt to the top layer of the melt. The Y123 crystal grows continuously as long as the nutrient Y211 exists. In this method, convection in the melt is an important factor in controlling the distribution of Y atoms in the melt, as is seen from the high Schmidt number of the melt ($Sc \cong 7000$). It is well known that the quality of substrates depends on the conditions for crystal growth such as the crystal pulling rate and temperature distribution on the wall of the crucible. Therefore it is very important to understand melt motion, and fluctuation of temperature in the melt to obtain bigger and higher quality single crystal. Studies on the dynamic patterns of convection in a Czochralski melt are numerous. However, a detailed convective flow pattern in the melt for the Y123 single crystal growth process has not yet been clearly presented.

A recent publication of Namikawa *et al.* [8] shows some results of numerical calculation for steady state melt convection. However, the numerical results obtained by Szmyd *et al.* [12, 13] for similar boundary conditions show periodically oscillating convection, and it was found that

thermal boundary condition seriously affect the instability of the melt flow [11, 14]. A recent work of Yamauchi *et al.* [19] shows that unsteady three-dimensional computation is required for the detailed analysis of the melt flow of the Y123 production process by Czochralski method. However, unsteady 3-D computation of the concentration field of Y atoms is too expensive and highly unstable because allocation of a large number of grid points is necessary to grasp thin concentration boundary layer near the crucible wall. Therefore, in this study, numerical computation of the flow, thermal and Y atoms concentration fields in the melt are performed for the yttrium barium copper oxide superconductor (YBa_2Cu3O_{7-x}) single crystal growth by the Czochralski method assuming the steadiness of the melt flow. Additionally, the present computation will be made assuming axisymmetry of the fields. Yamauchi *et al.* [19] also shows that velocity and thermal fields retain axisymmetry when they remain steady. These conditions can actually be realized at a very slow pulling-up speed of seed crystal or at rather small rotating speed and small temperature difference between the bottom and top of the crucible side wall. Calculations are presented for a buoyancy/crystal-rotation driven combined convection flow regime.

2. Formulation and numerical scheme

The geometry of the numerical calculations for the yttrium concentration is shown in Fig. 4. A crystal with radius R_x grew from the cylindrical melt in a crucible with radius R_c and depth H_l. The melt is bounded at the top around the center by a coaxially mounted crystal which rotates with angular velocity Ω_x. The melt free surface around the crystal is assumed to be flat and free from surface tension effect. The crystal interface is assumed to be kept at temperature T_x, and Y concentration is assumed to be constant there at an equilibrium concentration level $C = C_x(T_x)$ [6, 18] (see Fig. 5). Temperature and Y concentration at the bottom of the melt are assumed respectively to be T_c, and $C = C_c(T_c)$ [6, 18] (see Fig. 5). Melt flow is assumed to be axisymmetric. The fluid is considered to be incompressible, Newtonian, Boussinesque and its properties are taken to be constant. Material properties and dimensions for the melt adopted in the calculations are listed in Table 1.

The governing equations to be solved are the conservation laws for total fluid mass, momentum, enthalpy and Y concentration. For incompressible flows, these laws can be written with cylindrical–polar co-ordinates as follows:

- total fluid mass conservation equation: continuity equation

$$\frac{\partial U_r}{\partial r} + \frac{U_r}{r} + \frac{\partial U_z}{\partial z} = 0 \tag{1}$$

- momentum conservation equation: Navier–Stokes equation:

$$\frac{\partial U_r}{\partial t} + U_r \frac{U_r}{\partial r} - \frac{U_\varphi^2}{r} + U_z \frac{\partial U_r}{\partial z} = -\frac{1}{\rho}\frac{\partial P}{\partial r} + \nu\left(\frac{\partial^2 U_r}{\partial r^2} + \frac{1}{r}\frac{\partial U_r}{\partial r} - \frac{U_r}{r^2} + \frac{\partial^2 U_r}{\partial z^2}\right) \tag{2a}$$

$$\frac{\partial U_\varphi}{\partial t} + U_r \frac{U_\varphi}{\partial r} + \frac{U_r U_\varphi}{r} + U_z \frac{\partial U_\varphi}{\partial z} = \nu\left(\frac{\partial^2 U_\varphi}{\partial r^2} + \frac{1}{r}\frac{\partial U_\varphi}{\partial r} - \frac{U\varphi}{r^2} + \frac{\partial^2 U_\varphi}{\partial z^2}\right) \tag{2b}$$

$$\frac{\partial U_z}{\partial t} + U_r \frac{U_z}{\partial r} + U_z \frac{\partial U_z}{\partial z} = -\frac{1}{\rho}\frac{\partial P}{\partial z} + \nu\left(\frac{\partial^2 U_z}{\partial r^2} + \frac{1}{r}\frac{\partial U_z}{\partial r} + \frac{\partial^2 U_r}{\partial z^2}\right) + g\beta(T - T_m) \tag{2c}$$

- thermal energy conservation equation

$$\rho C_p\left(\frac{\partial T}{\partial t} + U_r \frac{\partial T}{\partial r} + U_z \frac{\partial T}{\partial z}\right) = \lambda\left[\frac{1}{r}\frac{\partial}{\partial r}\left(r\frac{\partial T}{\partial r}\right) + \frac{\partial^2 T}{\partial z^2}\right] \tag{3}$$

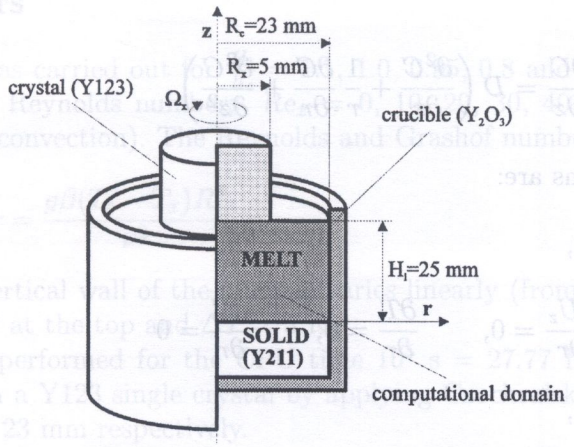

Fig. 4. The geometry of the numerical calculations

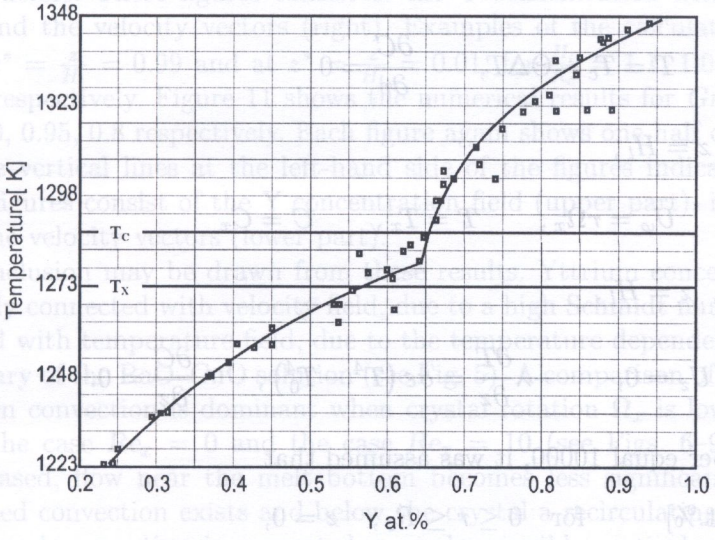

Fig. 5. Solution limit of the Y elements in the solvent along the Y123–$3BaCuO_2 \cdot 2CuO$

Table 1. Dimension and thermophysical data applied in the calculation for the melt of Y123 single crystal growth

PROPERTY		VALUE	
crystal radius	R_x	0.005	m
crucible radius	R_c	0.023	m
melt depth	H_l	0.025	m
density of melt	ρ	5500	kg/m^3
dynamic viscosity of melt	μ	4×10^{-2}	kg/(m s)
thermal expnsion coefficient	β	2.6×10^{-4}	1/K
specific heat	C_p	579.71	J/(kg K)
thermal conductivity of melt	λ	2.2	W/(m K)
melting temperature	T_m	1272	K
acceleration of gravity	g	981	m/s^2
diffusion coefficient	D	1×10^{-9}	m^2/s

- concentration equation

$$\frac{\partial C}{\partial t} + U_r \frac{\partial C}{\partial r} + U_z \frac{\partial C}{\partial z} = D\left(\frac{\partial^2 C}{\partial r} + \frac{1}{r}\frac{\partial C}{\partial r} + \frac{\partial^2 C}{\partial z^2}\right) \tag{4}$$

The boundary conditions are:

- for $r = 0,\ 0 \le z \le H_l$,

$$U_r = U_\varphi = 0, \qquad \frac{\partial U_z}{\partial r} = 0, \qquad \frac{\partial T}{\partial r} = 0, \qquad \frac{\partial C}{\partial r} = 0$$

- for $0 \le r \le R_c,\ z = 0$,

$$U_r = U_z = 0, \qquad T = T_c, \qquad C = C_c$$

- for $r = R_c,\ 0 \le z \le H_l$,

$$U_r = U_z = 0, \qquad T = T_c - \Theta\Delta T, \qquad \frac{\partial C}{\partial r} = 0$$

- for $0 \le r \le R_x,\ z = H_l$,

$$U_r = U_z = 0, \qquad U_\varphi = r\Omega_x, \qquad T = T_x, \qquad C = C_x$$

- for $R_x \le r \le R_c,\ z = H_l$,

$$\frac{\partial U_r}{\partial z} = \frac{\partial U_\varphi}{\partial z} = U_z = 0, \qquad -\lambda\frac{\partial T}{\partial z} = \sigma\varepsilon\left(T^4 - T_0^4\right), \qquad \frac{\partial C}{\partial z} = 0.$$

For Grashof number equal 10000, it was assumed that

$C_c = 0.67393$ [Y at.%] for $0 \le r \le R_c,\ z = 0$,

$C_x = 0.55720$ [Y at.%] for $0 \le r \le R_x,\ z = H_l$,

where $\Theta = \frac{z}{H_l}$ and ΔT is the temperature difference between the bottom and the top of the crucible vertical wall, σ is the Stefan–Boltzmann constant ($\sigma = 5.6667 \times 10^{-8}$ W/(m^{2}K^4)), ε is the emissivity from the surface ($\varepsilon = 0.7$) and temperature $T_o = 1243$ K. The concentration buoyancy effect is negligible due to a low yttrium concentration in the BaO–CuO melt. Y concentration in the melt is of the order of 3.65 kg/m^3 at the melt surface and 3.76 kg/m^3 at the melt bottom (density of the melt $\rho = 5500$ kg/m^3). Therefore the term $g\beta_c(C - C_m)$ is almost two order of magnitude smaller than $g\beta(T - T_m)$ and can be assumed to be negligibly small. The flow, thermal and yttrium concentration fields in the melt were calculated numerically by the control-volume-based finite difference method [9], solving the finite-difference equivalents of the momentum, energy and concentration equations. Staggered grids were used for the velocity components. The SIMPLER algorithm [9] was used to solve the pressure. The central finite difference approximation was applied for the diffusion terms while, for the convection terms, the QUICK scheme [7] was used. The present scheme was based on fully implicit discretization schemes taking into account the unsteady terms of governing equations. The ADI (Alternative-Direction-Implicit method) [10] was combined in the iterative procedure at each time step to solve the algebraic equations. The grid points were uniformly allocated in $r-z$ plane and total number of grid points was 96×104. The time step was $\Delta t^* = 10^{-6}$, where t^* is non-dimensional time $t^* = \frac{t\nu}{R_x^2}$.

3. Numerical results

Numerical computation was carried out for $\frac{H_l}{R_c} = 1.1, 1.0, 0.95, 0.8$ and for Grashof number $Gr = 10000$, for seven different Reynolds numbers, $Re_x = 0, 10, 20, 30, 40, 50, 60$ (for $Re_x = 0$ the problem is one of natural convection). The Reynolds and Grashof numbers are defined as

$$Re_x = \frac{(R_x^2 \Omega_x)}{\nu}, \qquad Gr = \frac{g\beta(T_c - T_x)R_c^3}{\nu^2}.$$

The temperature of the vertical wall of the crucible varies linearly (from $z = 0$ to $z = H_c$) from T_c at the bottom to $T_c - \Delta T$ at the top and $\Delta T = 3$ K.

The calculations were performed for the CPU time 10^5 s = 27.77 hours. In practice, it takes about two weeks to obtain a Y123 single crystal by applying Czochralski method if H_l and R_c are assumed to be 25mm and 23 mm respectively.

Figures 6, 7, 8 and 9 illustrate some examples of the numerical results for $Gr = 10000$, $Re_x = 0$, 10, 20, 30, 40, 50, and for $\frac{H_l}{R_c} = 1.1, 1.0, 0.95, 0.8$ respectively. Each figure shows one-half of the vertical section of the melt, and the vertical lines at the left-hand side of the figures indicate the centre line of the crucible. These figures consist of the Y concentration field (left), isotherms of the melt (middle) and the velocity vectors (right). Examples of the calculated Y distribution in BaO–CuO melt at $z^* = \frac{z}{H_l} = 0.99$ and at $z^* = \frac{z}{H_l} = 0.01$, for $\frac{H_l}{R_c} = 1.1, 1.0, 0.95, 0.8$ are shown in Figs. 10 and 12, respectively. Figure 11 shows the numerical results for $Gr = 10000$, $Re_x = 60$, and for $\frac{H_l}{R_c} = 1.1, 1.0, 0.95, 0.8$ respectively. Each figure again shows one-half of the vertical section of the melt, and the vertical lines at the left-hand side of the figures indicate the centre line of the crucible. These figures consist of the Y concentration field (upper part), isotherms of the melt (central part) and the velocity vectors (lower part).

The following conclusion may be drawn from these results. Yttrium concentration field in Ba–Cu–O melt is strongly connected with velocity field, due to a high Schmidt number in the melt, and is strongly connected with temperature field, due to the temperature dependence of Y solubility at the solid wall boundary of the BaO–CuO solution (see Fig. 5). A comparison of figures demonstrates that thermally driven convection is dominant when crystal rotation Ω_x is low, there is almost no difference between the case $Re_x = 0$ and the case $Re_x = 10$ (see Figs. 6–9). When the crystal rotation Ω_x is increased, flow near the melt bottom becomes less significant. Near the top free surface outward forced convection exists and below the crystal a recirculating flow is incurred. On the other hand, natural convection is generated near the crucible vertical wall by the buoyancy force. As the crystal rotation Ω_x is increased the forced convection becomes stronger and yttrium distribution in the BaO–CuO melt becomes more uniform (see Figs. 6–9).

Figures 10, 11 and 12 present other interesting results. As the melt depth H_l decreases, Y distribution in BaO–CuO melt becomes non-uniform below the crystal ($z^* = \frac{z}{H_l} = 0.99$) and at the bottom of the melt ($z^* = \frac{z}{H_l} = 0.01$) for $Re_x = 60$. This is a consequence of the flow structure below the crystal where upflow appears close to the axis of the crucible. When the melt depth is decreased from $\frac{H_l}{R_c} = 1.1$ to $\frac{H_l}{R_c} = 0.8$, a strong upflow becomes to prevail below the whole crystal and produces a steep temperature gradient (see Fig. 11). Then, the interface temperature is increased and yttrium distribution becomes non-uniform in the BaO–CuO melt below the crystal (see Fig. 10) and at the bottom of the melt (see Fig. 12). As evidently seen in Fig. 10, the crystal rotation should be reduced with decreasing the melt depth in order to keep a nearly uniform yttrium distribution below the crystal.

4. Conclusions

Numerical computations of the yttrium distribution in the BaO–CuO melt were performed for single crystal growth of the yttrium barium copper oxide superconductor ($YBa_2Cu_3O_{7-x}$) by the Czochralski method. The flow in the melt was assumed to be axisymmetric and was modelled as

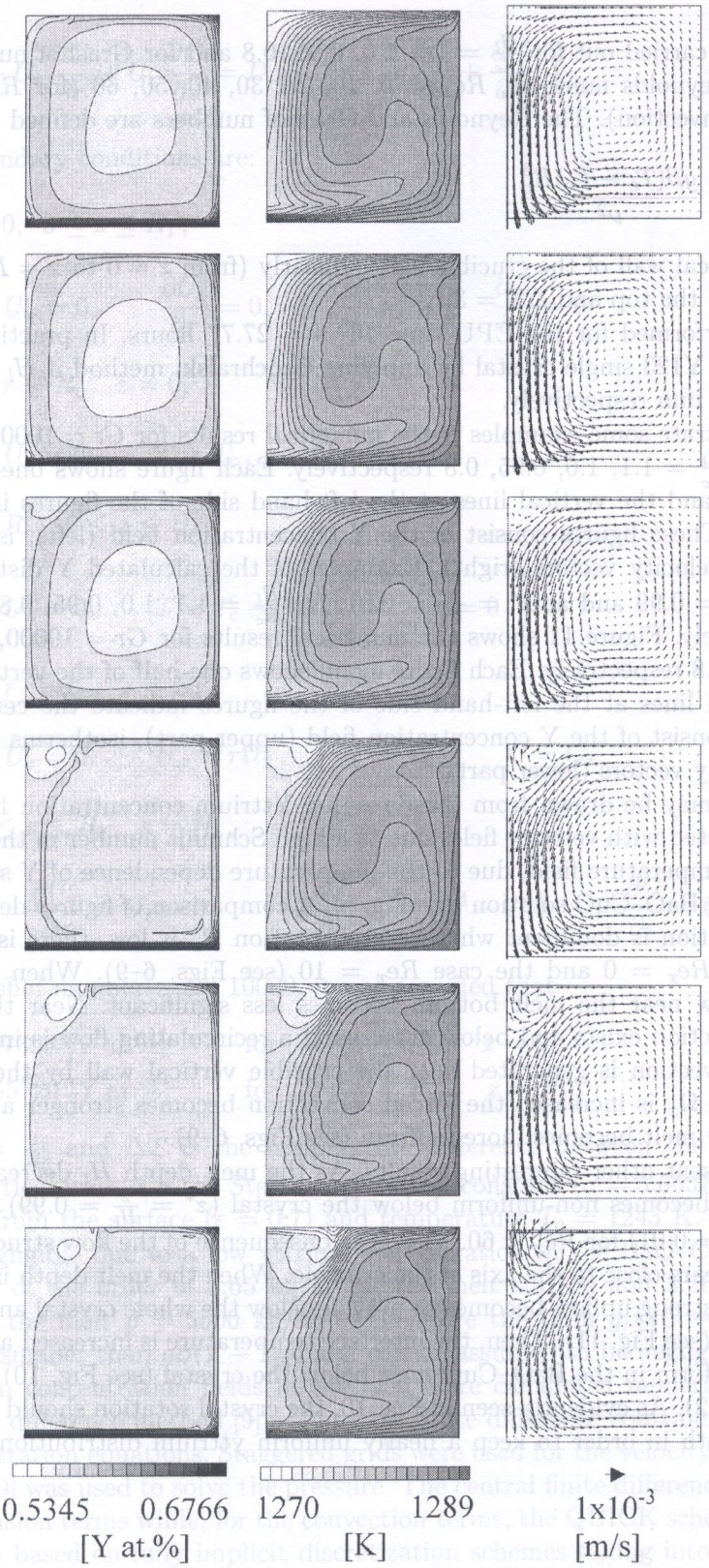

Fig. 6. Y distribution in Ba–Cu–O melt, isotherms and velocity vectors for $Gr = 10000$ and $Re_x = 0,\ 10,\ 20,\ 30,\ 40,\ 50$ ($\frac{H_l}{R_c} = 1.1$)

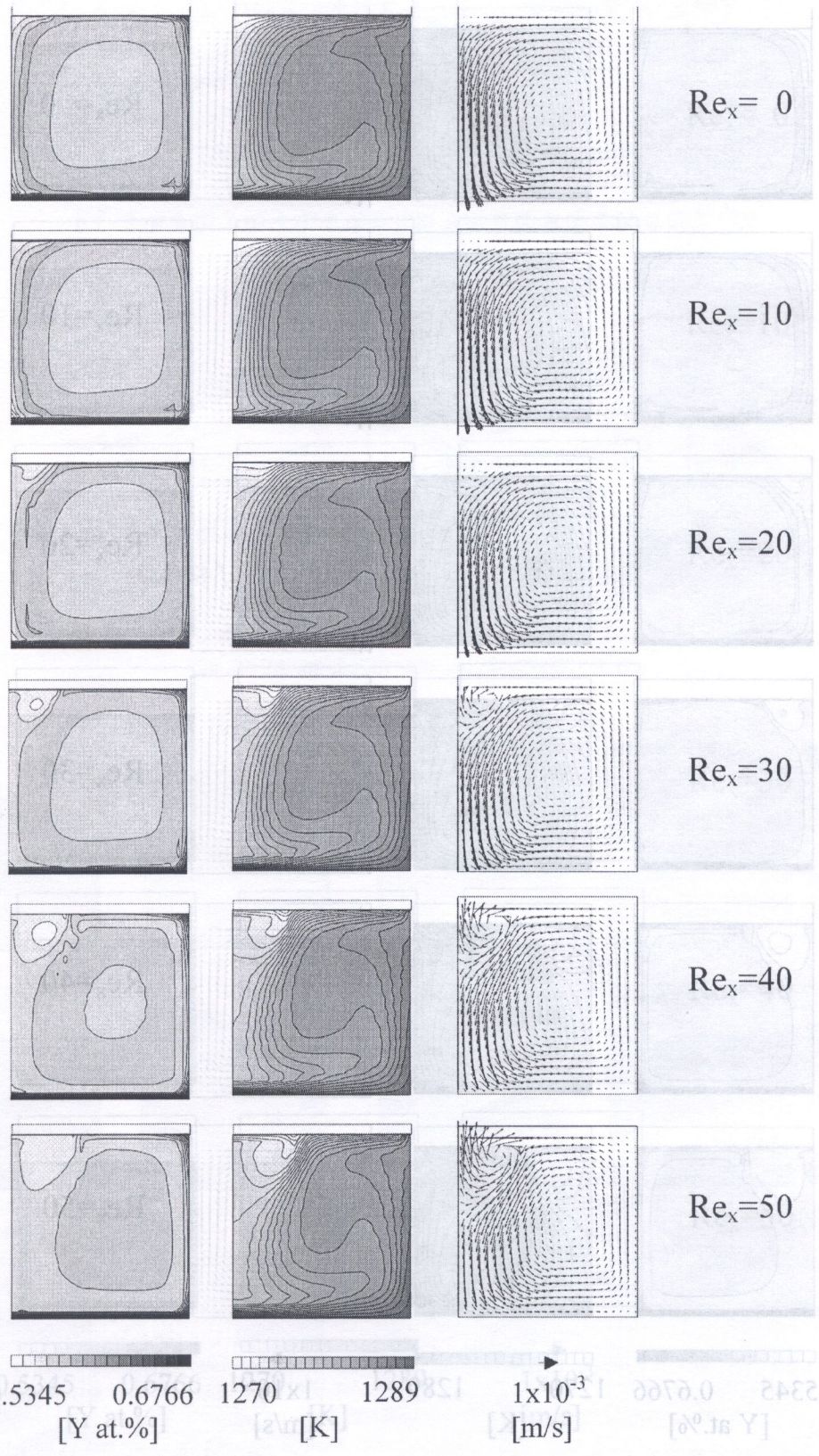

Fig. 7. Y distribution in Ba–Cu–O melt, isotherms and velocity vectors for $Gr = 10000$ and $Re_x = 0, 10, 20, 30, 40, 50$ ($\frac{H_l}{R_c} = 1.0$)

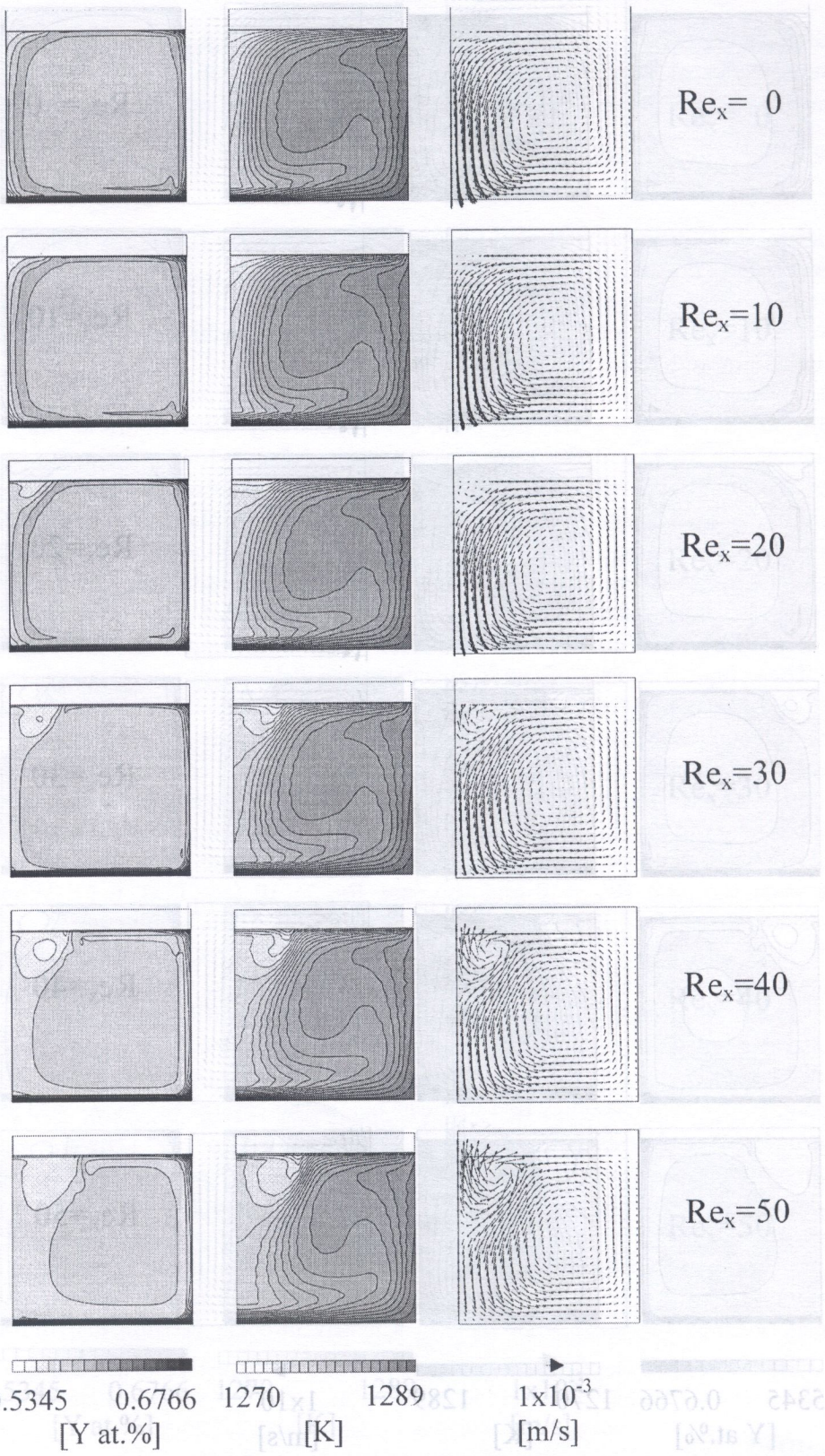

Fig. 8. Y distribution in Ba–Cu–O melt, isotherms and velocity vectors for $Gr = 10000$ and $Re_x = 0, 10, 20, 30, 40, 50$ ($\frac{H_l}{R_c} = 0.95$)

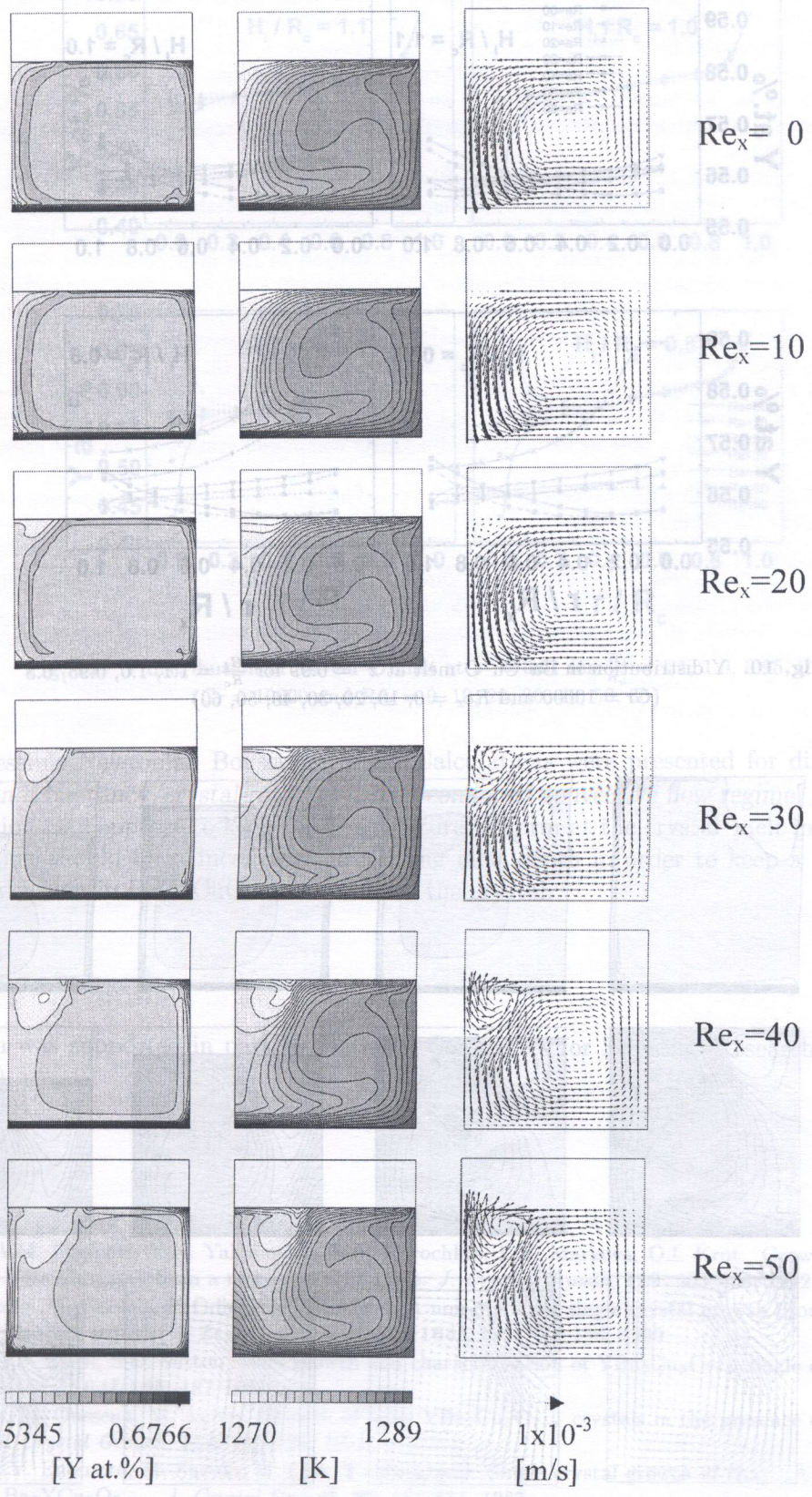

Fig. 9. Y distribution in Ba–Cu–O melt, isotherms and velocity vectors for $Gr = 10000$ and $Re_x = 0, 10, 20, 30, 40, 50$ ($\frac{H_l}{R_c} = 0.8$)

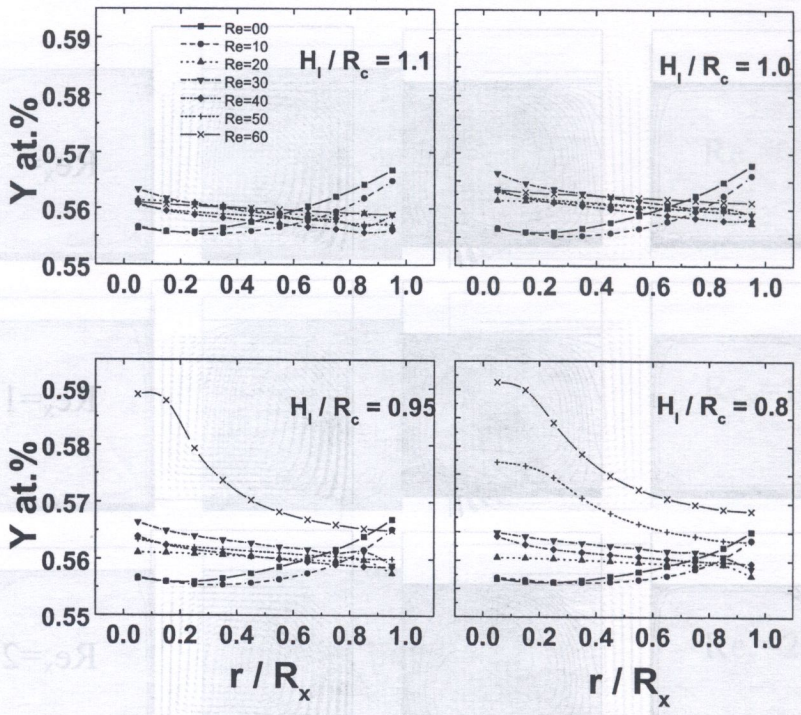

Fig. 10. Y distribution in Ba–Cu–O melt at $z^* = 0.99$ for $\frac{H_I}{R_c} = 1.1, 1.0, 0.95, 0.8$ ($Gr = 10000$ and $Re_x = 0, 10, 20, 30, 40, 50, 60$)

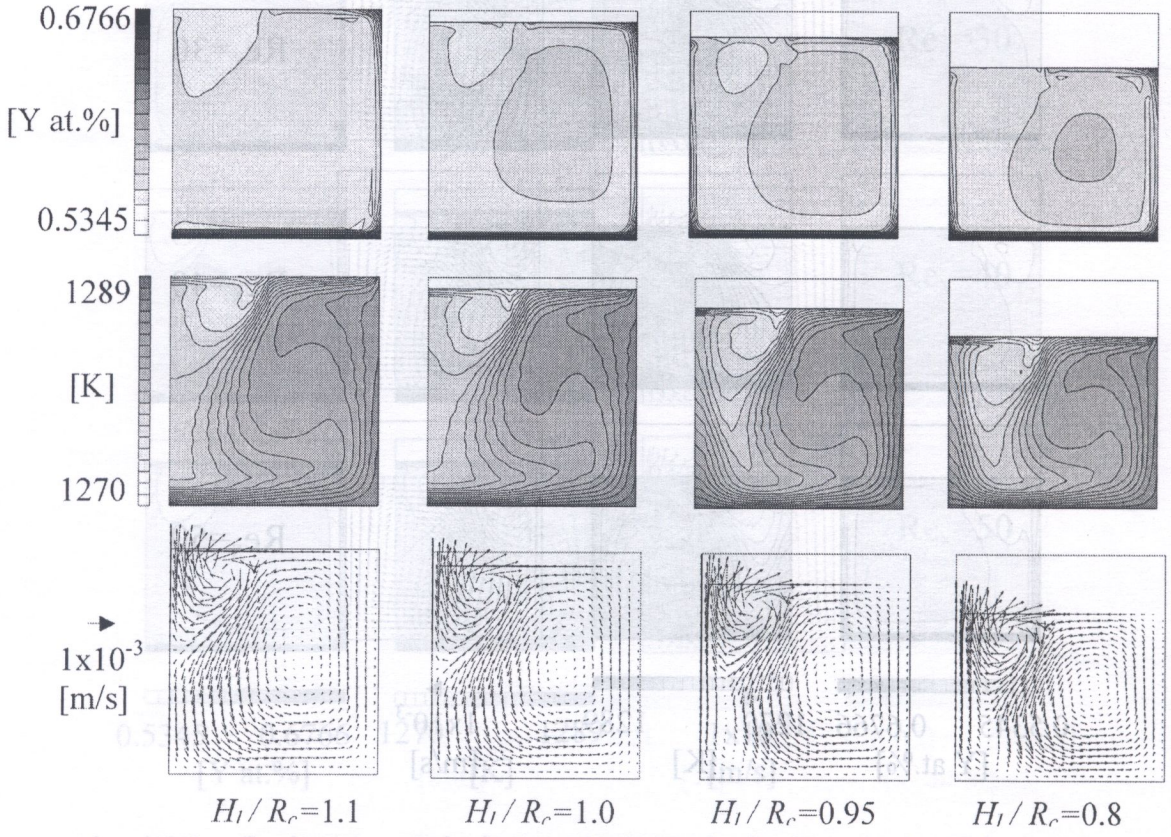

Fig. 11. Y distribution in Ba–Cu–O melt, isotherms and velocity vectors for $Gr = 10000$, $Re_x = 60$ ($\frac{H_I}{R_c} = 1.1, 1.0, 0.95, 0.8$)

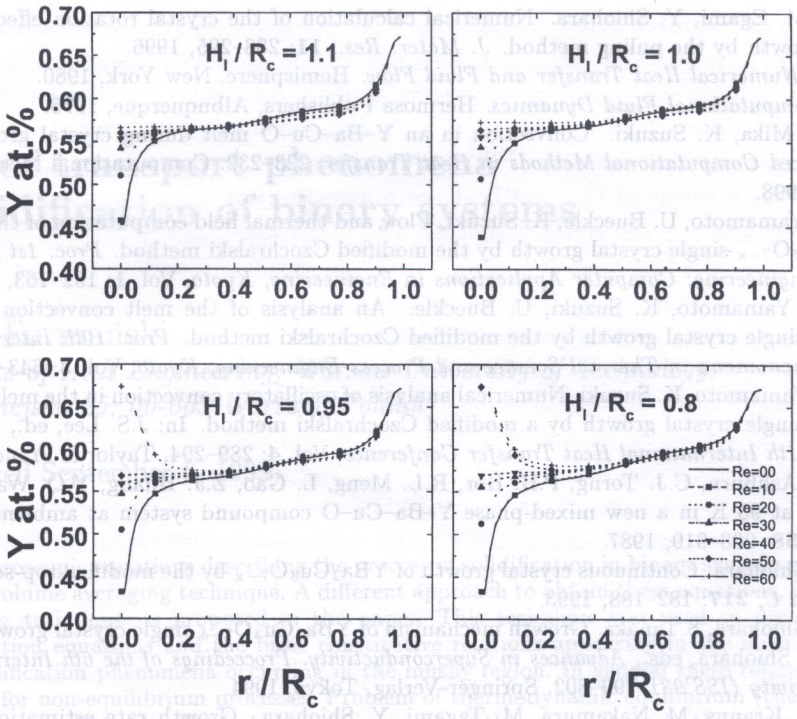

Fig. 12. Y distribution in Ba–Cu–O melt at $z^* = 0.01$ for $\frac{H_l}{R_c} = 1.1, 1.0, 0.95, 0.8$ ($Gr = 10000$ and $Re_x = 0, 10, 20, 30, 40, 50, 60$)

an incompressible Newtonian Boussinesq fluid. Calculations were presented for different levels of melt depth in a buoyancy/crystal-rotation driven combined convective flow regime. An appropriate crystal rotation rate appears to keep the temperature uniform at the crystal–melt interface and the crystal rotation should be reduced with decreasing melt depth in order to keep a nearly uniform yttrium distribution in BaO–CuO solution below the crystal.

Acknowledgements

This research was supported in part by National Committee for Scientific Research, (Grant KBN 7T08B00916).

References

[1] S.N. Barilo, A.P. Ges, S.A. Guretskii, D.I. Zhigunov, A.V. Zubets, A.A. Ignatenko, A.N. Igumentsev, I.D. Lomako, A.M. Luginets, V.N. Yakimovich, L.A. Kurochkin, L.V. Markova, O.I. Krot. Growth of bulk single crystals of $YBa_2Cu_3O_{7-x}$ from a new type of crucible. *J. Crystal Growth*, **119**: 403–406, 1992.

[2] K. Dembinski, M. Gervais, P. Odier, J.P. Coutures. A non polluting single crystal growth process for YBaCuO and phase diagram studies. *J. Less-Common Metals*, **164&165**: 177–186, 1990.

[3] A. Drake, J.S. Abell, S.D. Sutton. Flux growth and characterisation of $YBa_2Cu_3O_{7-x}$ single crystals. *J. Less-Common Metals*, **164&165**: 187–192, 1990.

[4] R. Gagnon, M. Oussena, M. Aubin. Growth of large $YBa_2Cu_3O_{7-x}$ crystals in the presence of a temperature gradient. *J. Crystal Growth*, **114**: 186–190, 1991.

[5] Y. Hikada, Y. Enomoto, M. Suzuki, M. Oda, T. Murakami. Single crystal growth of $(La_{1-x}A_x)_2CuO_4$ (A=Ba or Sr) and $Ba_2YCu_3O_{7-y}$. *J. Crystal Growth*, **85**: 581–584, 1987.

[6] Ch. Krauns, M. Sumida, M. Tagami, Y. Yamada, Y. Shiohara. Solubility of RE elements into Ba–Cu–O melts and enthalpy of dissolution. *Phys. B*, **96**: 207–212, 1994.

[7] B.P. Leonard. A stable and accurate convective modelling procedure based on quadratic upstream interpolation. *Compt. Meths. Appl. Mech. Eng.*, **19**: 59–98, 1979.

[8] Y. Namikawa, M. Egami, Y. Shiohara. Numerical calculation of the crystal rotation effect on $YBa_2Cu_3O_{7-x}$ single crystal growth by the puling method. *J. Mater. Res.*, **11**: 288–295, 1996.

[9] S.V. Patankar. *Numerical Heat Transfer and Fluid Flow.* Hemisphere, New York, 1980.

[10] P.J. Roache. *Computational Fluid Dynamics.* Hermosa Publishers, Albuquerque, 1976.

[11] J.S. Szmyd, G. Mika, K. Suzuki. Convection in an Y–Ba–Cu–O melt during crystal growth by Czochralski method. *Advanced Computational Methods in Heat Transfer*, 223–232. Computational Mechanics Publications, Southampton, 1998.

[12] J.S. Szmyd, T. Yamamoto, U. Bueckle, K. Suzuki. Flow and thermal field computation of the melt for superconductor $YBa_2Cu_3O_{7-x}$ single crystal growth by the modified Czochralski method. *Proc. 1st JSPS–NUS Seminar on Integrated Engineering; Computer Applications in Engineering, Kyoto*, Vol. **1**: 152–163, 1996.

[13] J.S. Szmyd, T. Yamamoto, K. Suzuki, U. Bueckle. An analysis of the melt convection for superconductor $YBa_2Cu_3O_{7-x}$ single crystal growth by the modified Czochralski method. *Proc. 10th International Symposium on Transport Phenomena in Thermal Science and Process Engineering, Kyoto*, Vol. **3**: 643–648, 1997.

[14] J.S. Szmyd, T. Yamamoto, K. Suzuki. Numerical analysis of oscillatory convection in the melt for superconductor $YBa_2Cu_3O_{7-x}$ single crystal growth by a modified Czochralski method. In: J.S. Lee, ed., *Heat Transfer 1998. Proceedings of 11th International Heat Transfer Conference*, Vol. **4**: 289–294, Taylor & Francis, Levittown, 1998.

[15] M.K. Wu, J.R. Ashburn, C.J. Torng, P.H. Hor, R.L. Meng, L. Gao, Z.J. Huang, Y.Q. Wang, C.W. Chu. Superconductivity at 93 K in a new mixed-phase Y–Ba–Cu–O compound system at ambient pressure. *Physical Review Letters*, **58**: 908–910, 1987.

[16] Y. Yamada, Y. Shiohara. Continuous crystal growth of $YBa_2Cu_3O_{7-x}$ by the modified top-seeded crystal pulling method. *Physica C*, **217**: 182–188, 1993.

[17] Y. Yamada, Y. Shiohara, S.Tanaka. Growth mechanism of $YBa_2Cu_3O_{7-\delta}$ single crystal grown by crystal pulling. In: T. Fujita, Y. Shiohara, eds., *Advances in Superconductivity. Proceedings of the 6th International Symposium on Superconductivity (ISS'93)*, 799–802, Springer-Verlag, Tokyo, 1994.

[18] Y. Yamada, Ch. Krauns, M. Nakamura, M. Tagami, Y. Shiohara. Growth rate estimation of $YBa_2Cu_3O_{7-x}$ single crystal growth by crystal pulling. *J. Mater. Res.*, **10**(7): 1601–1604, 1995.

[19] T. Yamauchi, G. Mika, J.S. Szmyd, K. Suzuki. Unsteady tree-dimensional melt flow computation of Czochralski single crystal growth of super-conducting material. (to be published).